Size-Controlled Synthesis of Machinable Single Crystalline Gold Nanoplates

Chil Seong Ah, Yong Ju Yun, Hyung Ju Park, Wan-Joong Kim, Dong Han Ha, and Wan Soo Yun*

Electronic Devices Group, Korea Research Institute of Standards and Science, Daejeon 305-600, Korea

Received June 8, 2005. Revised Manuscript Received August 8, 2005

Monodispersive size-controlled gold nanoplates were synthesized with high purity from the reduction of hydrogen tetrachloroaurate by reduced amount of sodium citrate, which kinetically controls the reaction pathway, in the presence of poly(vinyl pyrrolidone) (PVP). With the insufficient addition of the reductant, the molar ratio of sodium citrate and PVP relative to hydrogen tetrachloroaurate played an important role in determining the geometric shape and size of the product. These nanoplates were single crystals with planar width of 80−500 nm and thickness of 10−40 nm, exhibiting strong surface plasmon absorption in the near-infrared (NIR) region of 700−2000 nm. The gold nanoplates were used as the synthetically provided nanoblocks to fabricate single-crystalline nanocomponents, such as a nanoscaled gear or a nanoscaled letter.

1. Introduction

Inorganic nanoparticles exhibit a wide range of optical and electrical properties that depend strongly on both size and shape[1−3] and are of interest as nanoscaled building blocks, templates, and components in chemical/biological sensors and electronic/optical devices.[4−6] In the last several years, many groups have concentrated on shape-controlled metal nanostructures, such as prisms, rods, wires, cubes, belts, and even branched multipods, and have often achieved a high yield.[3,7−11] Besides, it has long been a pursuit in the development of nanotech research to apply the synthetically provided "bottom-up" nanoblocks to the "top-down" device and system.[12,13] Nanoparticles, wires, and tubes were adopted in the demonstration of various functional devices, bringing the advent of nanoscience and technology,[5,6,14] while the application of the nanocrystals to micro/nanoelectromechanical systems is strongly restricted so far. Planar thin nanoparticles, or nanoplates, which were originally observed as a residual byproduct in the synthesis of spherical nanoparticles, have attracted a growing interest in materials research[15−17] and can be a promising candidate in this approach of post-synthesis shaping of the nanocrystals. Since they can also exhibit size-dependent surface plasmon absorption in the visible−near-infrared (vis-NIR) region, the synthesis of size-controlled gold nanoplates with good purity and yield is of great importance in a wide range of applications in nanoscience and technology. Herein, we report on the synthesis of the size- and shape-controlled single-crystalline gold nanoplates in high yield and purity with a narrow size distribution by chemical reduction of hydrogen tetrachloroaurate by a reduced amount of sodium citrate, which kinetically adjusts the reaction pathway to a stepwise self-seeding growth of the nanoplates. Also, we demonstrate machining of the nanoplates to form nanocomponents of arbitrary shape, such as a nanogear and a nanoletter.

2. Experimental Section

Gold nanoplates were synthesized as follows. An aqueous solution of 250 mL of 1 mM $HAuCl_4$ was heated for 30 min with stirring. Then various amounts of 250 mM poly (vinyl pyrrolidone) (PVP) (molar ratio between the repeating unit of PVP and $HAuCl_4$ was from 0 to 8) were added, and then 3.75 mL of 34 mM sodium citrate (the molar ratio of sodium citrate to $HAuCl_4$ was 0.5) was quickly added. After refluxing for 1 h, the solution was collected and then filtered through an Isopore membrane filter after precipitation at room temperature. Gold nanocomponents, such as a nanogear or a nano-printing type were fabricated out of gold nanoplates using 30 kV and 1 pA Ga^+ FIB (focused ion beam) equipment (Dual Beam (SEM/FIB) system: Nova 200 Nanolab). The total etching time was 2 min for the nanocomponent fabrication.

* Corresponding author: e-mail wsyun@kriss.re.kr; tel +82-42-868-5952; fax +82-42-868-5953.

(1) Alivisatos, A. P. *Science* **1996**, *271*, 933.
(2) Link S.; El-Sayed, M. A. *J. Phys. Chem. B* **1999**, *103*, 8410.
(3) Jin, R.; Cao, Y. C.; Hao, E.; Metraux, G. S.; Schatz, G. C.; Mirkin, C. A. *Nature* **2003**, *425*, 487.
(4) Xia, Y.; Yang, P.; Sun, Y.; Wu, Y.; Mayers, B.; Gates, B.; Yin, Y.; Kim, F.; Yan, H. *Adv. Mater.* **2003**, *15*, 353.
(5) Park, S.-J.; Taton, T. A.; Mirkin, C. A. *Science* **2002**, *295*, 1503.
(6) Duan, X.; Huang, Y.; Cui, Y.; Wang, J.; Lieber, C. M. *Nature* **2001**, *409*, 66.
(7) Sau, T. K.; Murphy, C. J. *Langmuir* **2004**, *20*, 6414.
(8) Sun, Y.; Xia, Y. *Adv. Mater.* **2002**, *14*, 833.
(9) Sun, Y.; Xia, Y. *Science* **2002**, *298*, 2176.
(10) Sun, Y.; Mayers, B.; Xia, Y. *Nano Lett.* **2003**, *3*, 675.
(11) Chen, S.; Wang, Z. L.; Ballato, J.; Foulger, S. H.; Carroll, D. L. *J. Am. Chem. Soc.* **2003**, *125*, 16186.
(12) Chung, S.-W.; Ginger, D. S.; Morales, M. W.; Zheng, Z.; Chandrasekhar, V.; Ratner, M. A.; Mirkin, C. A. *Small* **2005**, *1*, 64.
(13) Sheehan, P. E.; Lieber, C. M. *Nanotechnology* **1996**, *7*, 236.
(14) Javey, A.; Guo, J.; Wang, Q.; Lundstorm, M.; Dai, H. *Nature* **2003**, *424*, 654.
(15) Sun, X.; Dong, S.; Wang, E. *Angew. Chem.* **2004**, *116*, 6520.
(16) Millstone, J. E.; Park, S.; Shuford, K. L.; Qin, L.; Schatz, G. C.; Mirkin, C. A. *J. Am. Chem. Soc.* **2005**, *127*, 5312.
(17) Shankar, S. S.; Rai, A.; Ankamwar, B.; Singh, A.; Ahmad, A.; Sastry, M. *Nat. Mater.* **2004**, *3*, 482.

10.1021/cm051225h CCC: $30.25
Published on Web 09/17/2005

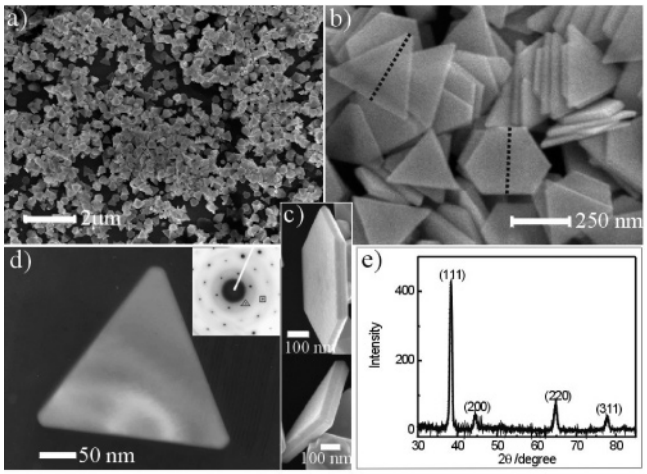

Figure 1. (a) Low- and (b) high-magnification SEM images of gold nanoplates. The "width" is defined as the vertical internal bisector line and the opposite straight line between two edges in the case of triangles and hexagons, respectively (dotted lines). (c) FE-SEM images of edges of individual hexagonal and triangular gold nanoplates. The edge of the nanoplates is not vertical but slightly tilted. (d) TEM image of an individual triangular Au nanoplate. The inset shows a diffraction pattern recorded by aligning the electron beam perpendicular to the triangular face of the nanoplate. In the [111] zone axis, the diffracted spots are indexed to {220} (boxed spot) and 1/3{422} (triangled spot) Bragg reflections, corresponding to lattice spacing 1.44 and 2.50 Å, respectively. (e) XRD pattern of the same batch of sample, confirming the crystal structure of fcc gold. The molar ratios of the reducing agent and the repeating units of PVP to $HAuCl_4$ were 0.5 and 5, respectively.

3. Results and Discussion

Low- and high-magnification field emission−scanning electron microscopy (FE-SEM) images of the gold nanoplates with an average width and thickness of 310 and 28 nm, respectively, are shown in parts a and b of Figure 1, respectively. The width and thickness of the nanoplates were measured in FE-SEM and transmission electron microscopy (TEM) images. These plates are comparatively monodispersive, either triangular or hexagonal, and comprised only of pure gold (Figure 1 and Supporting Information Figures S1 and S2). The edge of the plate is slightly tilted, reflecting the stability of specific facets of the nanocrystal (Figure 1c), and the surface of the plate is very flat (Supporting Information Figure S3). A TEM image of an individual gold nanoplate and convergent beam electron diffraction (CBED) pattern are shown in Figure 1d, supporting the single crystallinity of the nanoplate (Supporting Information Figure S4). The hexagonal nature of the diffraction spots clearly indicates that the thin nanoplates are highly [111] oriented with the flat top normal to the electron beam. An additional set in the ED pattern, corresponding to 1/3{422} with a 2.5 Å spacing, is also observed. The XRD pattern recorded from the same sample batch is also displayed in Figure 1e. It is worth noting that the intensity ratios of the (200) and (220) peaks to the (111) peak were much lower than the bulk value (0.1 and 0.17 versus 0.52 and 0.32), indicating that these nanoplates were dominated by {111} facets.

The size of the gold nanoplates was controlled by changing the concentration of PVP, while the molar ratio of the reducing agent to $HAuCl_4$ was kept at 0.5 (Figure 2a−d). When the molar ratio of the repeating unit of PVP to $HAuCl_4$ is increased from 0.1 to 8, the width and the thickness of the nanoplates increase from 96 and 14 to 450 and 39 nm, respectively (Figure 2d−a). Color change of the reaction mixture, attributable to the formation of nanoplates, occurred over a long period of time with increasing PVP concentration, meaning a slowdown of the nucleation and growth of the plates.[18] It seems that the size of the nanoplate was determined by the relative amount of the nuclei[19] that were initially formed by the reduction by sodium citrate, with respect to the remaining gold ions that were not fully reduced to Au^0: the fewer the initial nuclei, the larger the resulting nanoplates. The size of the nanoplates is also found to be dependent upon the molar ratio of sodium citrate to $HAuCl_4$. As the molar ratio of sodium citrate to $HAuCl_4$ was changed from 0.7 to 0.3 while the molar ratio of the repeating unit of PVP to $HAuCl_4$ was fixed at 5, the size of the nanoplates was increased (Supporting Information Figure S5). In this case also, the color change occurred slowly in the larger plate case. As inferred from the reaction rate (color change), the number of nuclei in solution decreases with either increasing PVP or decreasing citrate concentration. Figure 2e shows

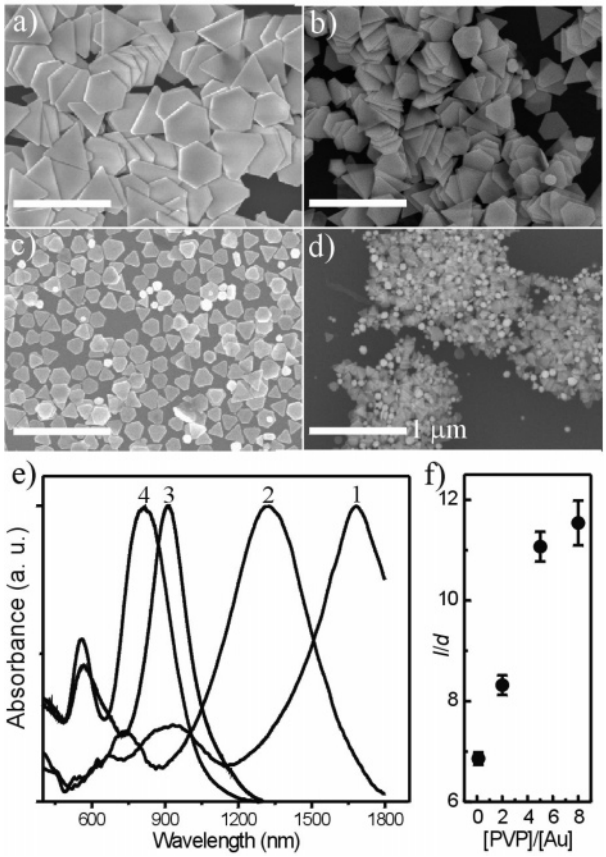

Figure 2. (a−d) FE-SEM images of gold nanoplates with average width and thickness of 450 ± 29 and 39 ± 4 nm (a), 310 ± 25 and 28 ± 3 nm (b), 158 ± 13 and 18 ± 3 nm (c), and 96 ± 12 and 14 ± 2 nm (d). Molar ratio of the repeating unit of PVP (MW ≈ 55 000, $n \approx 500$) to $HAuCl_4$ was 8:1 (a), 5:1 (b), 2:1 (c), and 0.1:1 (d). Scale bar is 1 μm. (e) UV−vis−NIR absorption spectra of the samples in panels a−d). Spectra 1−4 were obtained from the corresponding samples a−d. The solutions of larger gold nanoplates were suspended in D_2O for the absorption measurement to avoid the absorption due to H_2O. (f) Aspect ratio (width/thickness) as a function of the molar ratio of PVP to Au.

(18) Pastoriza-Santos, I.; Liz-Marzan, L. M. *Langmuir* **2002**, *18*, 2888.
(19) Brown, K. R.; Walter, D. G.; Natan, M. J. *Chem. Mater.* **2000**, *12*, 306.

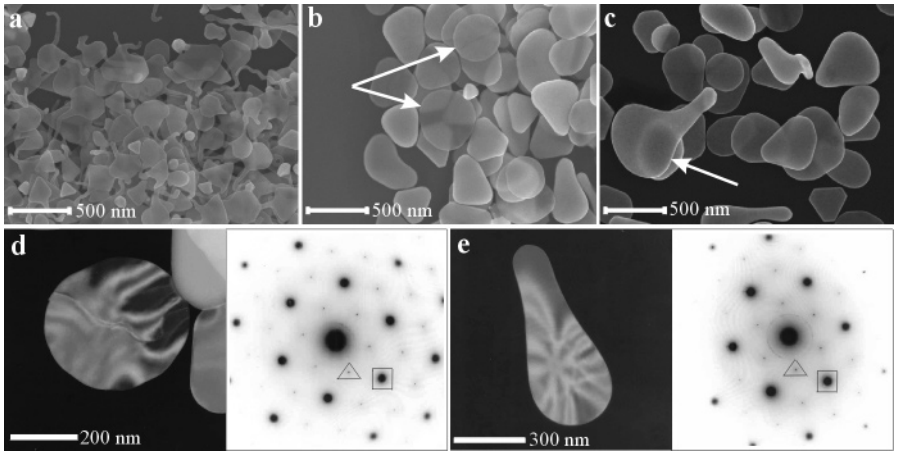

Figure 3. FE-SEM and TEM images and ED patterns of gold nanoplates synthesized without PVP. (a−c) FE-SEM images of an Au colloid before (a), 100 s after (b), and 1 h after (c) addition of a reducing agent. Coin-like (b) and irregularly shaped (c) Au nanoplates are indicated by arrows. The molar ratio of sodium citrate to $HAuCl_4$ was 0.5. (d, e) TEM image and ED pattern of (d) a coin-like and (e) an irregularly shaped gold nanoplate. In the [111] zone axis, the diffracted spots are indexed to {220} (boxed spot) and 1/3{422} (triangled spot) Bragg reflections, corresponding to lattice spacing 1.44 and 2.5 Å, respectively.

the UV−vis−NIR absorption spectra of the samples described in Figure 2a−d. For each sample, the distinct absorption peak in the longer wavelength region is attributed to in-plane dipole plasmon resonance of gold nanoplates. The out-of-plane dipole resonance ~530 nm is sufficiently weak that it is barely discernible. Other peaks in the spectra are considered to be the contribution of multipole resonances (for example, a broad band at 732 of spectrum 2 or at 930 nm of spectrum 1, which could be assigned to be the in-plane quadrupole modes of gold nanoplates).[16] As shown in Figure 2e, a size-sensitive in-plane dipole plasmon absorption band of the nanoplates shifted from red to NIR region with increasing width of the nanoplates (4 to 1 in Figure 2e).

Since the aspect ratio (width to thickness) of the nanoplates increases with increasing plate size (Figure 2f), we can assume that the remaining gold ions undergo autocatalytic reduction on the preferred surfaces of the initial nuclei,[20] since the reduction potential of gold ion on the gold surface becomes positive compared to the case of atom [Au_{metal}/Au^I (+1.68 V) and Au_{atom}/Au^I (−1.5 V)].[21] Then the formation of the nanoplates can be a result of kinetically preferred growth in the lateral direction of the small gold nuclei. When the molar ratio of sodium citrate to $HAuCl_4$ is higher than 1, the product was dominated by nanoparticles with irregular or spherical shape. We believe that a small amount of sodium citrate, as in the case of our experiments, produces a small number of nuclei in the solution and leaves a sufficient amount of gold ions that can take part in the further growth of the nuclei by heterogeneous reaction on the preferred surface, leading to the lateral growth of the nuclei, that is, the growth of the nanoplates. No detectable gold ions are remaining in the solution at the end of the reaction, indicating the complete incorporation of gold ions onto the nanoplates.

Figure 3 shows that gold nanoplates can also be formed without the addition of PVP if only the reductant is not sufficiently added into the reaction mixture. In this case, the molar ratio of sodium citrate to $HAuCl_4$ was 0.5. The circumference of nanoplates, however, was very irregular in this case compared to the triangular or hexagonal nanoplates prepared with the PVP. In the earlier stage of the reaction (Figure 3a), round-shaped or stingray-like plates appeared. After completion of the reaction (parts b and c of Figure 3), coin-like or irregularly shaped rounded nanoplates were formed. Parts d and e of Figure 3 show the TEM image and CBED pattern, respectively. The electron diffraction pattern was obtained by directing the electron beam perpendicular to the planar face of the nanoplate. The hexagonal nature of the diffraction spots clearly indicates that the planar surfaces of the nanoplates, regardless of the synthetic condition, are {111}-faceted. From the comparison between Figures 1, 2, and 3, we can conclude that PVP leads the formation of triangular or hexagonal plates with relatively monodisperse size distribution, as well as that the insufficient addition of reductant is the key parameter driving the formation of the gold nanoplates.

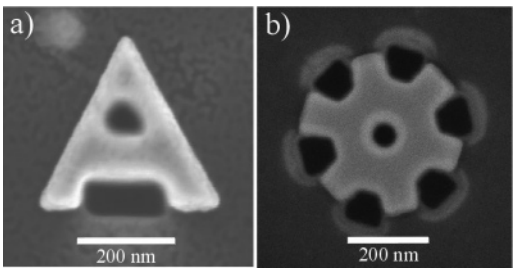

Figure 4. (a) Nanoletter, and (b) nanogear fabricated out of gold nanoplates.

These gold nanoplates can be used as single-crystalline substrates for the fabrication of arbitrary-shaped nanocomponents by postmachining. Figure 4 shows examples of the nanocomponents. A nanoletter and a nanogear were fabricated by focused ion beam (FIB) machining of the gold nanoplates prepared by the above-described chemical synthesis. The single-crystalline nanogear may be transferred to another place for further fabrication of nano-assembly. The nanoletter could be regarded as the smallest printing type. To our knowledge, this is the first example of machining a synthetically provided nanoblock to nanoscaled

(20) Petroski, J. M.; Wang, Z. L.; Green, T. C.; El-Sayed, M. A. *J. Phys. Chem. B* **1998**, *102*, 3316.
(21) Jana, N. R.; Gearheart, L.; Murphy, C. J. *Chem. Mater.* **2001**, *13*, 2313.

components, which might be useful in the realization of nanoelectromechanical systems and in the fundamental studies of metal nanostructures. We are sure that much more complexed nanocomponents, such as nanowheels, nanosaws, etc., which may pave the way to the realization of nano/micro-machines, can also be fabricated out of the nanoplates.[22]

4. Conclusions

On adjusting the reaction rates by insufficient addition of the reductant, the reaction proceeds in a two-step manner with self-seeding that results in the formation of planar nanocrystals or nanoplates with high yield and purity. Roles of reductant and surfactant in the nanoplate growth are explained with systematic experimental data. By varying the amount of those reagents, we were able to control the shape and size of the single-crystalline nanoplates with a narrow distribution, exhibiting strong size-dependent surface plasmon absorption in the vis-NIR region. Furthermore, some interesting and arbitrary-shaped nanocomponents were fabricated out of the nanoplates by applying a lithographic method, which can be an example of the convergence of "top-down" and "bottom-up" approaches in the nanotechnology development. The {111}-faceted single-crystalline gold nanoplate provided by this work can be an excellent platform for molecular self-assembly, promising NIR absorbers,[23] and a key component in nano/biosensors and cancer hyperthermia,[24] as well as an excellent substrate for nanomachining.

Acknowledgment. This work is supported by the R&D Program for Fusion Strategy of Advanced Technologies. We thank Mee Jeong Kang for TEM studies.

Supporting Information Available: Figures showing low- and high-resolution TEM images, an AFM image, an X-ray energy dispersive spectrum, and a spectrum of width of gold nanoplates as a function of the molar ratio between sodium citrate and Au. This material is available free of charge via the Internet at http://pubs.acs.org.

CM051225H

(22) Yun, Y. J.; Ah, C. S.; Ha, D. H.; Yun, W. S. Manuscript in preparation.

(23) Shankar, S. S.; Rai, A.; Ahmad, A.; Sastry, M. *Chem. Mater.* **2005**, *17*, 566.
(24) Hirsch, L. R.; Stafford, R. J.; Bankson, J. A.; Sershen, S. R.; Rivera, B.; Price, R. E.; Hazle, J. D.; Halas, N. J. *Proc. Natl. Acad. Sci. U.S.A.* **2003**, *100*, 13549.